Residual Stress Evaluation: RES Computing System

T. Belà
CISE Tecnologie Innovative SpA, Milan, Italy
S. Ghia
ENEL-CRTN, Milan, Italy
C. E. Sampietri
CISE Tecnologie Innovative SpA, Milan, Italy

ABSTRACT

The two-dimensional finite element computing system RES, for non-linear thermal and mechanical problems, is presented. RES system was developed in order to analyze the problems concerning welding or quenching on the basis of state and phase change phenomena.
The simulation of two welding between pipes (6" and 28") has been performed to validate the computing system.
The computed results are compared with the experimental ones.
This work was carried out under an ENEL-CISE collaboration programme.

INTRODUCTION

Residual stresses, following welding and/or heat treatment processes for plant component assembling, are undesirable effects which can at times limit the component performance if operated in certain conditions. Experimental methods to evaluate the residual stress distribution through-the thickness are generally, although valuable, expensive and time consuming (Shack, 1980). In an attempt at overcoming the experimental method difficulties, the welding process simulation was extensively studied in the past decade with special attention paid to the problem occuring in BWR power plants; efforts were devoted to predict residual stress distribution in welded pipes (Rybicki, 1978; Rybicki, 1979; Brust, 1981).
These kinds of processes differ from the typical non-linear thermomechanical transient in that they require the analysis of state and phase changes. As a consequence the problem becomes higly non-linear and the accomplishment of "special purpose" computer code is necessary.
The aim of the paper is at presenting a computing system for the evaluation of residual stresses along with the results obtained from analyses of different pipe geometries.

COMPUTING SYSTEM DESCRIPTION

Although from a theoretical point of wiew the thermal and the mechanical problems are coupled, the real interaction between the two phenomena is very weak and the two problems are assumed to be uncoupled. Therefore it is also possible to perform a sequential analysis using two different computer codes; the results of the thermal code being the input data for the mechanical code.
Under these assumption computing system was built up which consists of the two finite element computer codes:
ATEN-2D (for the thermal problem) and ASFOR-2D (for the mechanical one) (Bon, 1986; Bon, 1987). The main characteristics of the thermal code are the following:

- all the material properties (e.g. thermal conductivity, specific heat, density) can vary with temperature
- three alternative methods are implemented in the code to modelize the state change phenomena (heat capacity discontinuity, enthalpic model, fictitious heat source method)
- the model of phase transformation is based on the use of IT diagrams.

The mechanical code inplements a thermoelastic-plastic model with the following charcteristics:

- all material properties (e.g., Young's modulus, yield stress, etc.) can vary with temperature
- the thermal plasticity part of the model utilizes the Von Mises yield function with a combined isotropic-kinematic hardening
- tension cut-off can be used to keep the stress state limited; the mean hydrostatic tension may depend on the temperature
- the trasformation strain (due to phase transformation) is given due account in the model.

NUMERICAL ANALYSES

Numerical analyses were performed to evaluate the reliability of the computational system and to obtain a deeper quantitative understanding of the welding processes. The computing system was used to analyze two pipe-welding experiments.

The first simulation was concerned with the welding of a 6-inch schedule 80 type 304 staniless steel pipe. In this case the influence of the magnitude of the heat input on the residual stress was examinad.

The second simulation considered the welding of a 28-inch schedule 80 type 304 stainless steel pipe.

For this pipe, in particular, the influence of the last pass on the final stress state was studied.

Residual stress calculation of 6 inch diameter pipe

The geometrical configuration of the experimental set-up is shown in Fig. 1. The welding was realized with five passes. The welding parameters are reported in literature (Ghia, 1986). The arc efficiency, which was experimentally unknown, was assumed to be equal to 0.75.

From a previous analysis (Belà, 1987) it was found that for pipes with small thicknesses the final stress state is mainly determinated by the two last welding passes. Therefore, in order to obtain a considerable computational saving, the above-stated consideration was applied to the present analysis. The five-pass finite element model and the positions of some thermocouples, used in the experimental test, are shown in Fig. 2. The model had 132 parabolic elements and 445 nodes. The assumed temperature-dependent properties (thermal and mechanical) of the material are reported in literature (Belà, 1988).

For each simulated layer the following boundary conditions was considered:

- heat flux applied to the puddle
- radiative and convective heat transfer on the outside surface
- corrective heat transfer on the inside surface.

The experimental and calculated temperature transients for the last pass relevant to thermocouples 1 and 2 are shown in Figs 3 and 4: crosses are the experimental data and the solid line is the numerical solution. The agreement between the experimental and numerical results is quite good. About the mechanical aspect of the problem, the same mesh shown in Fig. 2 was used for the simulation. The symmetry condition was imposed along the londitudinal direction while no constrain was considered in the radial direction.

In Fig. 5 the experimental set-up is reported. The experimental and numerical results for the axial stress are shown in Fig. 6: crosses are the values of the straingauges (Ghia, 1984) and squares are the numerical results evaluated in the Gauss points of the mesh. The experimental results are relevant to the four different angular positions along the pipe circumference (Fig. 5) and show

a nonaxi-symmetric behaviour of the weld. Solid and dashed lines are the best fit of calculated and experimental data and represent the residual stress profile across the pipe thickness.
The agreement between the numerical and experimental results is satisfactory.
The hoop stress shown a similar behaviour.
In order to examine the influence of the thermal input magnitude on the formation of the residual stress, the welding simulation was repeated with other two different values of the arc efficiency (η). In the first case the thermal input was reduced by 15% by assuming a value equal to 0.65 for η.
In fig. 7 the results (axial residual stresses) for the two values of the thermal input are compared. Crosses are the results for $\eta = 0.65$ and squares are the results for $\eta = 0.75$. The residual stress profile across the thickness undergoes wide variation. When $\eta = 0.65$ the inner surface shows tensile stress, whereas when $\eta = 0.75$ there is conpressive stress.
In the second case the thermal input was increased by 15% by assuming a value equal to 0.85 for the arc efficiency. In fig. 8 the comparison between the residual stress results is shown. Increase in thermal input produces increase in the compressive values.

Residual stress calculation of a 28 inch diameter pipe

The pipe geometry is plotted in Fig. 9. The experimental parameters are reported in the literature (Ghia, 1986) and the weld pass sequence is shown in Fig. 10.
In order to reduce the computational task the welding process was supposed to be symmetric respect to the weld centerline and the passes were groupped to form seven layers. The layers effectively simulated are dashed in the same Fig. 10.
The finite element discretization (152 parabolic elements) of the last pass and the thermocouples positions are shown in Fig. 11. The imposed boundary conditions were just described in the previous analysis.
The experimental and calculated temperature transients for the last pass, relevant to thermocouple 1, is shown in Fig. 12: triangles are the experimental data and solid line is the numerical solution. The agreement is very good.
For the mechanical evaluation, the same mesh was used. The experimental and numerical results for the axial residual stress are reported in Fig. 13 and represent the stress profile across the thickness at 5 mm. from the edge of the weld. The bars on the figure denote the effect of data collection at different angular position along the pipe circumference.
The comparison between the numerical and experimental results is satisfactory.
It can be noticed that the welding process induced a tensile residual stress at the inner surface of the pipe and this charachteristic is an important drawback because it can induce integranular stress corrosion craking and crack propagation.
It is stated in the literature that use of the last pass heat sink welding process (LPHSW) can prevent IGSCC by producing compressive residual stresses in the heat effected zones at the inner pipe surface (Battelle, 1981).
Therefore, the simulation of the welding process was repeated in order to verify the effectiveness of the method. In this case the thermal input was almost tripled and the convective heat transfer coefficient was increased to simulate the cooling water in the cavity.
The numerical results for the axial stress versus thickness are reported in Fig. 14. The comparison between this figure and the one obtained with the conventional welding process shows that the LPHSW produces a compressive stress state at the inner surface in the heat affected zone.

CONCLUSIVE REMARKS

This study was carried out with two goals:
- firstly, to verify the reliability of the developed computing system in predicting residual stress distributions;
- second, to get a deeper quantitative understanding of the phenomena and, in particular, of the influence of the last pass on the final stress state.

As for as the first goal is concerned, the numerical results are in quite good agreement with the experimental ones.
As for the second goal, the residual stress analyses suggested that the residual stress distribution depends on the heat input of the last pass. However, this phenomena decreases as the diameter is increased.

REFERENCES

Shack, W.S., Ellingson, W.A., Pahis, L.E. (1980). Measurements of Residual Stresses in Type 304 Stainless Steel Piping Butt Weldments. EPRI NP-1413.

Rybicki, E.F., Schmueser, D.W., Stonesifer, R.B., Groom, J.T., Mishler, H.W. (1978). A Finite Elements Model for Residual Stresses and Deflections in Girth-Butt Welded Pipes. Journal of Pressure Vessel Technology (ASME), Vol. 100, pp. 256-262.

Rybicki, E.F., Stonesifer, R.B., (1979). Computation of Residual Stresses due to Multipass Welds in Piping System. Journal of Pressure Vessel Technology (ASME), Vol. 101, pp. 149-154.

Brust, F.W., Rybicki, E.F., (1981). A computational Model of Becklay Welding for Controlling Residual Stresses in Welded Pipes. Journal of Pressure Vessel Technology (ASME), Vol. 103, pp. 226-232.

Bon, E., Nigro, L., Sampietri C. (1986). Problemi bidimensionali di conduzione del calore con cambiamenti di stato e di fase: il codice ATEN-2D. CISE 2991.

Bon, E., Nigro, L., Sampietri, C. (1987). Il codice ASFOR-2D per il calcolo delle tensioni residue in strutture bidimensionali. CISE 3497.

Ghia, S., Regis, V. (1986). Experimental and Analytical Residual Stresses Evaluation on 6" and 28" Buttwelded SS Pipe. EPRI Seminar on Countermeasures for pipe cracking in BWR'S, Palo Alto.

Belà, T., Sampietri, C. (1987). Applicazione del sistema di calcolo ATEN-2D, ASFOR-2D per la determinazione delle tensioni residue. CISE 4199.

Belà, T., Sampietri, C. (1988). Analisi parametrica della saldatura di una tubazione da 6". CISE 4545.

Ghia, S., Belà, T., Squilloni, A. (1984). Determinazione sperimentale del campo tensionale residuo in giunti saldati in AISI 304 per impieghi nucleari. XII Convegno Nazionale AIAS, Sorrento.

Battelle, Columbus Laboratories (1981). Controlling Residual Stresses by Heat Sink Welding. EPRI NP-2159-LD.

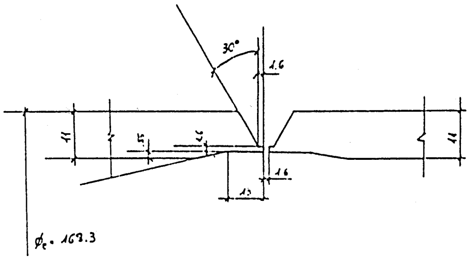

Fig. 1: Weld joint design for a 6 inch diameter pipe.

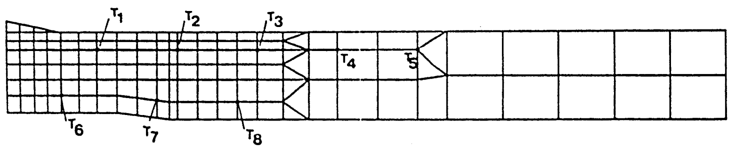

Fig. 2: Finite element grid for a 6 inch diameter pipe.

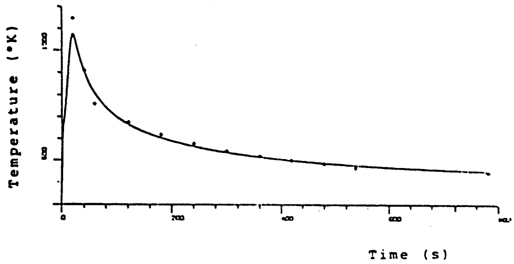

Fig. 3: Comparison of finite element results with experimental data (thermoc. n.1)

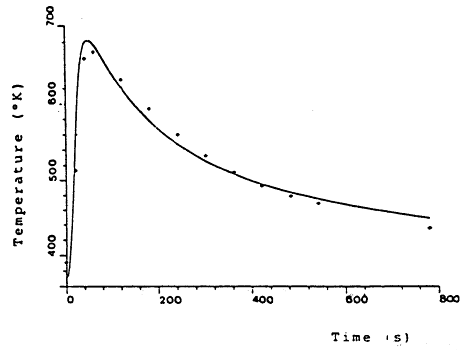

Fig. 4: Comparison of finite element results with experimental data (thermoc. n.2)

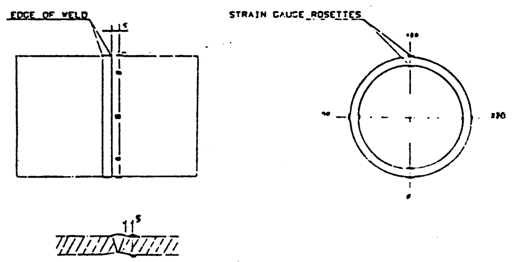

Fig. 5: Straingauge locations for residual stress measurements (6 inch pipe)

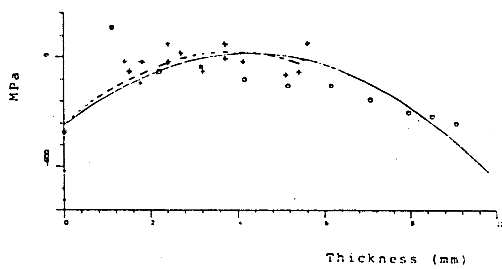

Fig. 6: Through-thickness axial residual stresses for 6 inch pipe (• calc., + exp.)

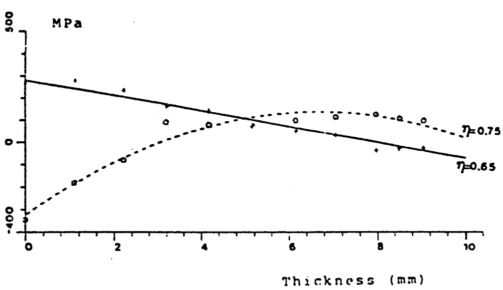

Fig. 7: Through-thickness axial residual stresses for 6 inch pipe (+η=0.65, ∘η=0.75)

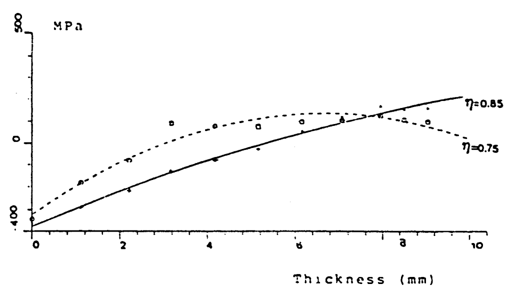

Fig. 8: Through-thickness axial residual stresses for 6 inch pipe (+η=0.85, ∘η=0.75)

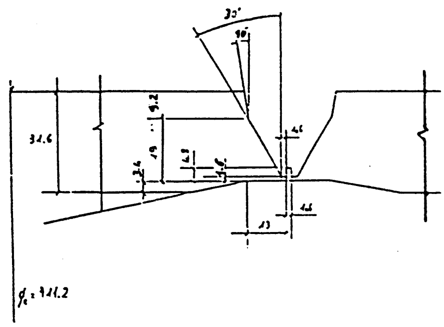

Fig. 9: Weld joint design for a 28 inch diameter pipe.

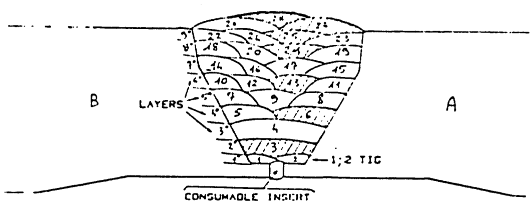

Fig. 10: Weld pass sequence for a 28 inch diameter pipe.

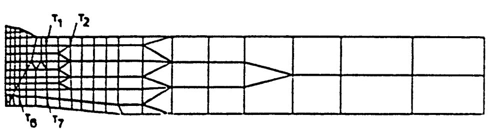

Fig. 11: Finite element grid for a 28 inch diameter pipe.

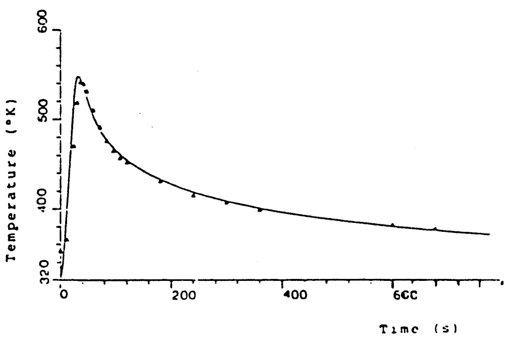

Fig. 12: Comparison of finite element results with experimental data (thermoc. n.1)

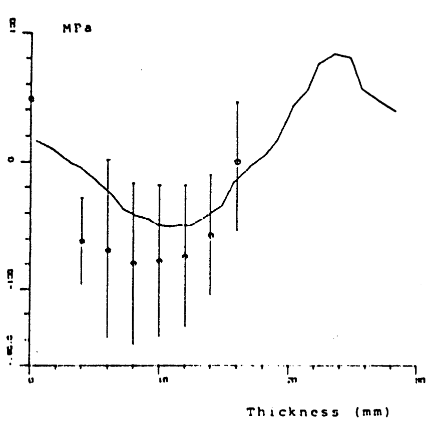

Fig. 13: Through-thickness axial residual stresses for 28 inch pipe (— calc., • exp.)

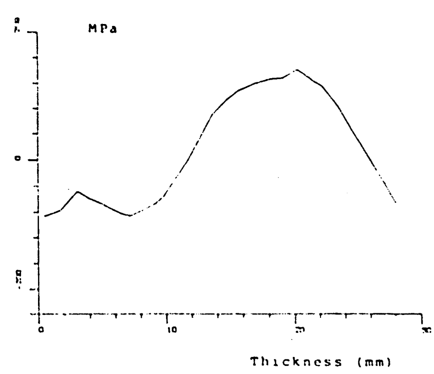

Fig. 14: Through-thickness axial residual stresses for 28 inch pipe (LPHSW)